Proteasome-mediated Proteolysis of the Polyglutamine-expanded Androgen Receptor Is a Late Event in Spinal and Bulbar Muscular Atrophy (SBMA) Pathogenesis*

Erin M. Heine[1], Tamar R. Berger[1], Anna Pluciennik, Christopher R. Orr, Lori Zboray, and Diane E. Merry[2]

From the Department of Biochemistry and Molecular Biology, Thomas Jefferson University, Philadelphia, Pennsylvania 19107

Background: Polyglutamine-expanded androgen receptor forms nuclear inclusions of cleaved AR.

Results: Soluble aggregates and insoluble inclusions of polyglutamine-expanded AR contain full-length AR, which becomes proteolyzed by the proteasome within maturing inclusions.

Conclusion: Proteolysis of the mutant AR is a late event in pathogenesis.

Significance: Therapeutic strategies for SBMA should target pathogenic events involving full-length AR protein.

Proteolysis of polyglutamine-expanded proteins is thought to be a required step in the pathogenesis of several neurodegenerative diseases. The accepted view for many polyglutamine proteins is that proteolysis of the mutant protein produces a "toxic fragment" that induces neuronal dysfunction and death in a soluble form; toxicity of the fragment is buffered by its incorporation into amyloid-like inclusions. In contrast to this view, we show that, in the polyglutamine disease spinal and bulbar muscular atrophy, proteolysis of the mutant androgen receptor (AR) is a late event. Immunocytochemical and biochemical analyses revealed that the mutant AR aggregates as a full-length protein, becoming proteolyzed to a smaller fragment through a process requiring the proteasome after it is incorporated into intranuclear inclusions. Moreover, the toxicity-predicting conformational antibody 3B5H10 bound to soluble full-length AR species but not to fragment-containing nuclear inclusions. These data suggest that the AR is toxic as a full-length protein, challenging the notion of polyglutamine protein fragment-associated toxicity by redefining the role of AR proteolysis in spinal and bulbar muscular atrophy pathogenesis.

Spinal and bulbar muscular atrophy (SBMA),[3] or Kennedy disease, is an X-linked, adult onset, slowly progressive neurodegenerative disease affecting men (1). SBMA results from a polyglutamine-encoding CAG trinucleotide repeat expansion in the first exon of the androgen receptor (AR) gene (2). The CAG repeat is polymorphic between normal individuals with disease resulting when the expansion is greater than 39 repeats (2). Patients manifest clinically with proximal limb and bulbar muscle atrophy and weakness, cramping, fasciculations, dysarthria, and dysphagia (1). Neuropathological studies of SBMA reveal a loss of motor neurons from the anterior horn of the spinal cord and brainstem motor nuclei (1, 3). In addition, remaining motor neurons manifest a salient pathological feature of ubiquitinated, nuclear inclusions (NI) composed mainly of truncated AR protein (4, 5).

SBMA is part of a family of inherited neurodegenerative diseases caused by expansion of a CAG-encoding polyglutamine tract; this family includes Huntington disease, several types of spinocerebellar ataxia, and dentatorubropallidoluysian atrophy (for a review, see Ref. 6). The gender specificity of SBMA is due not only to the X-linked location of the AR gene but also to the requirement for androgen binding to the mutant receptor for disease manifestation (7–10). While signs of androgen insensitivity are sometimes seen in SBMA, the disease is not due to a loss of AR function but rather to a gain of a toxic property of the mutant polyglutamine-expanded androgen receptor. Although the precise mechanistic pathway leading to AR misfolding, aggregation, and its subsequent toxicity has not been fully elucidated, it is known that binding of one of the natural AR ligands, testosterone or 5α-dihydrotestosterone, and nuclear localization are required for both motor dysfunction and neuropathology (9, 11, 12).

The NI observed in mouse and cell models of SBMA as well as in SBMA autopsy material are primarily detected with antibodies directed against N-terminal portions of the AR; antibodies detecting C-terminal epitopes failed to detect NI described in early studies (4, 5, 7, 13) (see Fig. 1A). Biochemical evidence from the analysis of a transgenic mouse model of SBMA (14) suggested that the absence of C-terminal epitopes is due to an aberrant proteolytic cleavage of the AR rather than to epitope masking of the misfolded protein. Support for the production of an insoluble cleaved polyglutamine-containing protein fragment can be found in human disease tissue and animal models of other polyglutamine disorders (15–17). Moreover, transgenic mice expressing a mutant N-terminal AR fragment (18) show substantially greater severity of disease symptoms than mice expressing full-length AR protein from the same promoter (7), suggesting a model in which cleavage of the AR pro-

motes the adoption of a misfolded, toxic, aggregation-prone conformation. However, the role of cleavage and the protease responsible for mutant AR proteolysis are still undetermined. Substantial evidence suggests that soluble, aggregated species of misfolded polyglutamine-expanded proteins are likely responsible for neuronal dysfunction and toxicity, whereas nuclear inclusions represent the sequestration of such species into non-toxic, neuroprotective entities (19–21). Nevertheless, the presence of inclusions containing aggregated polyglutamine species reveals the inability of the cell to efficiently degrade the misfolded protein and is indicative of a pathological process. Given this background, we hypothesized that the mutant AR is cleaved to form a toxic, soluble, N-terminal AR fragment and set out to understand the timing and location of mutant AR proteolysis. Such an understanding would likely reveal a new target for therapeutic intervention.

In our studies described here, we used a combination of imaging and biochemical approaches to reveal a novel view of the aggregation process in SBMA, one in which inclusions are formed from *full-length* AR protein and cleavage of the mutant AR occurs only after it is integrated into an inclusion. Our results also indicate that soluble aggregation species consist of full-length AR protein. Proteolysis of the mutant AR to produce the N-terminal fragments observed in nuclear inclusions is a late event, occurring after the mutant AR has already become SDS-insoluble. We show that ubiquitin is present on the same aggregated AR species that become proteolyzed, a process that we show requires proteasomal activity. Finally, the conformation-specific antibody 3B5H10, previously shown to predict risk of death in models of Huntington disease (22), bound to soluble, full-length mutant AR but not to proteolyzed AR fragments within inclusions, further challenging the idea that toxicity results from a toxic AR fragment in SBMA.

EXPERIMENTAL PROCEDURES

Construction of Double Labeled, Expanded Polyglutamine AR (DLAR)-expressing Cell Lines—DNA sequences encoding CFP-AR25Q-YFP, CFP-AR65Q-YFP, and CFP-AR121Q-YFP (a kind gift from Marc Diamond, Washington University School of Medicine, St. Louis, MO) were excised with NheI/FspI and ligated into the pTRE2 plasmid (Clontech) cut with NheI/EcoRV. To create single labeled YFP-tagged AR-encoding plasmids, the CFP/YFP-pTRE2-AR plasmids created above along with untagged pTRE2-AR plasmid were digested with NheI and BstBI, and the 5′- or 3′-AR-containing fragments were swapped. Transfection of Tet-On PC12 cells (Clontech) was executed with each CFP/YFP-pTRE2-AR or YFP-pTRE2-AR plasmid and a plasmid conferring hygromycin resistance (pTK-Hygro) using Lipofectamine with Plus Reagent (Invitrogen). Transfected cells were selected in the presence of 200 μg/ml hygromycin (Invitrogen), and single colonies were isolated and screened for AR protein expression by induction with 0.5 μg/ml doxycycline (Clontech). Positive clones were verified by Western blotting (using AR(H280) antibody) and by direct observation of fluorescence produced by the CFP and YFP tags. Genomic DNA was extracted from positive clones, and the CAG repeat length was verified by PCR and sequencing analy-sis. The concentration of doxycycline required to induce equivalent levels of AR protein between cell lines was determined.

Cell Culture Reagents—PC12 cells inducibly expressing human AR were maintained as described (13). AR expression was induced in cells containing double fluorescently labeled AR with 121 glutamines (DLAR121Q) or DLAR25Q with 10 ng/ml doxycycline or in cells containing unlabeled AR with 112 glutamines (AR112Q) or AR10Q with 500 ng/ml doxycycline. 5α-Dihydrotestosterone (DHT; Sigma) was resuspended in ethanol, and cells were treated with a final concentration of 10 nM DHT. Cells were treated with epoxomicin (Sigma-Aldrich) at 10, 25, or 50 nM (in dimethyl sulfoxide) for 48 h.

Dissolution of Inclusions—AR expression was induced in PC12 cells (AR112Q and AR10Q), and cells were treated with DHT (10 nM) for 7 days. Cells were lysed with radioimmune precipitation assay lysis buffer (50 mM Tris-HCl, pH 8.0, 0.15 M NaCl, 1% Nonidet P-40, 0.5% sodium deoxycholate, 0.1% SDS, and protease inhibitors), and 750 μg of protein from each cell line was incubated overnight at 4 °C with or without 1.5 μg of antibody (AR(H280) or AR(C19)). Capture of the immunoprecipitated AR was carried out using Protein G Dynabeads (Invitrogen) for 30–60 min at room temperature followed by separation from the unbound sample using a Dynal magnet. Each sample was split into 250- and 500-μg-equivalent portions (1:2 ratio). The 500-μg portion was treated with 100% formic acid while rotating for 15 min at 37 °C. The eluate was separated from the Dynabeads, evaporated overnight in a vacuum centrifuge, and resuspended in 2× Laemmli buffer. Sample pH was neutralized by adding 1–5 μl of 1.5 M Tris buffer, pH 8. The 250-μg portion was eluted from the Dynabeads with 2× Laemmli buffer, and samples were boiled for 5 min. Samples were evaluated by SDS-PAGE and Western blot using AR-318 (1:500). Following AR-318 detection, membranes were probed for rabbit IgG (using anti-rabbit secondary antibody) to identify the IgG heavy chain of the antibody used for immunoprecipitation.

Dissolution of Inclusions from YFP-tagged AR-expressing Cells—PC12 cells expressing AR112Q, AR with 111 glutamines fused with YFP at the C terminus (AR111Q-YFP), or AR25Q-YFP were grown for 10 days in the presence of 750 ng/ml doxycycline and 10 nM DHT and for an additional 2 days in the presence of 10 nM DHT. Cells were harvested and lysed with 2% SDS lysis buffer. AR inclusions were isolated by ultracentrifugation at 60,000 rpm for 2 h 45 min in a 70.1 Ti rotor at room temperature. Pellets were washed with 2% SDS lysis buffer and centrifuged again at 60,000 rpm for 2h 45 min. Pellets were either dissolved in 2× Laemmli buffer or treated with a 1:1 mixture of trifluoroacetic acid (Thermo Scientific) and 1,1,1,3,3,3-hexafluoro-2-propanol (Sigma-Aldrich) (TFA:HFIP) for 2 h at room temperature. TFA:HFIP was evaporated from the samples using a SpeedVac, the sample was dissolved in 2× Laemmli buffer, and the pH was adjusted with 1.5 M Tris-HCl, pH 8.8. Samples were resolved by 10% SDS-PAGE and transferred to PVDF membrane. The membrane was probed with anti-GFP (1:1000) (Clontech), AR(N-20) (1:1000) (Santa Cruz Biotechnology), or AR(441) (1:500) (Santa Cruz Biotechnology) antibody.

Immunofluorescence—PC12 cells, primary neuronal cultures, and mouse tissue sections were fixed and stained as described previously (11). Antibodies used included AR(H280) (1:100), AR(441) (1:50) (Santa Cruz Biotechnology), 3B5H10 (1:4000) (a kind gift from Steve Finkbeiner, Gladstone Institute of Neurological Disease), anti-FLAG antibody (1:100) (Pierce), and SMI32 (1:1000) (Sternberger Monoclonals Inc., Baltimore, MD). Immunostained cells were visualized using a Leica Microscope (Leica Microsystems GmbH, Wetzlar, Germany) and imaged using iVision Mac® software (BioVision Technologies, Exton, PA). Confocal images were captured using a Zeiss LSM 510 META confocal microscope and software (Carl Zeiss Microimaging, Inc., Thornwood, NY) and a NikonC1 Plus laser confocal microscope (Nikon Instruments Inc., Melville, NY).

SDS-Agarose Gel Electrophoresis (SDS-AGE)—Cells were harvested in 2% SDS lysis buffer (2% SDS, 10 mM Tris, pH 8, and 150 mM NaCl), and 100 μg of protein was diluted in non-reducing Laemmli sample buffer and boiled for 5 min. Samples were electrophoresed in agarose as described previously (23–26). Briefly, protein lysates were electrophoresed on a 12-cm-long, 8-mm-thick 1% agarose gel containing 0.1% SDS (in 375 mM Tris-HCl, pH 8.8) at 100 V at 4 °C. Proteins were transferred to a PVDF membrane at 200 mA for 1.5 h using a semidry transfer apparatus (Owl HEP Semidry Electroblotting Systems, Thermo Scientific) followed by Western analysis using antibody AR(441) (1:100), 3B5H10 (1:10,000), or AR(H280) (1:1000).

Live Cell Imaging—DLAR121Q PC12 cells were plated on poly-D-lysine-coated glass bottom dishes (MatTek Corp., Ashland, MA) and maintained as described (13). AR expression was induced with 10 ng/ml doxycycline, and cells were treated with 10 nM DHT (Sigma). After 72 h, medium was replaced with Opti-MEM I (Gibco) containing 12.5 mM additional HEPES (Sigma), 5% horse serum, 2.5% fetal bovine serum (Gibco), 10 ng/ml doxycycline, and 10 nM DHT. Each plate was then mounted on the Zeiss Axiovert 200M inverted microscope (Carl Zeiss Microimaging, Inc.), and each field was imaged in four 1-μm increments every 2 h for 20 h. Both YFP and CFP fluorescence emissions as well as differential interference contrast images were captured at each time point using MetaMorph image acquisition and analysis software (Molecular Devices, Inc., Sunnyvale, CA). 2-μm z-stacks were compiled as maximum intensity projection images for each time point and for each channel.

Generation of Adeno-associated Viruses—Adeno-associated viruses containing C-terminal FLAG-tagged human AR (111-CAG or 25-CAG) were created as described (27). Briefly, adeno-associated virus (AAV) cis plasmids carrying AR with 111 or 25 CAGs and containing N-terminal nuclear localization signal (NLS; ×3) to ensure nuclear localization were co-transfected with Trans (H21) and Adenovirus Helper (δ6) into HEK293T cells using calcium/phosphate transfection. After 5 days, cells were lysed by repeated freeze/thaw cycles to release viral particles followed by centrifugation to remove cellular debris. The optimum volume of cell lysate to attain effective and equivalent infection of motor neurons in primary dissociated spinal cord cultures was determined by serial dilution infections of primary cultures and immunostaining for AR (AR-318) and neurofilament heavy chain (SMI32) to identify motor neurons.

Primary Dissociated Spinal Cord Cultures and AAV Infection—Dissociated spinal cord cultures were established according to Roy *et al.* (28) with modifications as described (11, 29, 30). Briefly, spinal cords from non-transgenic 13.5-day-old mouse embryos were dissected on ice in dissection medium (0.1% dextrose, 2% sucrose, 6.8 mM NaCl, 0.27 mM KCl, 8.4 μM Na$_2$HPO$_4$, 11 μM KH$_2$PO$_4$, and 9.9 mM HEPES), pooled, dissociated with trypsin, plated on poly-D-lysine (Sigma)-coated German glass coverslips (Chemglass Life Sciences), and cultured for 3 weeks in glial conditioned medium (minimum essential medium, 3% charcoal-stripped horse serum, 35 mM NaHCO$_3$, 0.5% dextrose, 1% N3, 10 nM 2.5S nerve growth factor). After 3 weeks, cultures were transduced with AAV-NLS-AR111Q-FLAG or AAV-NLS-AR25Q-FLAG for 5 days followed by treatment with 10 μM DHT for 3–18 days. Cultures were then immunostained as described, and motor neurons were identified by size and morphology as well as immunoreactivity with an antibody (SMI32) detecting unphosphorylated neurofilament heavy chain. Experimental procedures utilizing mice were conducted according to the guidelines of the Office of Laboratory Animal Welfare and with the approval of the Thomas Jefferson University Institutional Animal Care and Use Committee.

Proteasome Inhibition—AR-containing PC12 cells were simultaneously treated with doxycycline to induce AR expression with 10, 25, or 50 nM epoxomicin (Sigma-Aldrich) (in dimethyl sulfoxide) and 10 nM DHT for 48 h. Cells were then fixed with 4% paraformaldehyde and immunostained for AR epitopes as described above.

Mouse Nuclear Extracts—Spinal cords were dissected from male transgenic mice expressing human AR with either 24 CAGs or 112 CAGs from the prion protein (PrP) promoter at 7.5 weeks ($n = 4$) and 11 months ($n = 4$) of age. Nuclear extractions were performed through homogenization of freshly dissected tissue in a hypotonic lysis buffer (10 mM HEPES, pH 7.9 at 4 °C, 1.5 mM MgCl$_2$, 10 mM KCl, and 0.5 mM DTT). Duplicate spinal cords were pooled, and the pooled lysates were centrifuged at 3000 × g for 10 min at 4 °C. The pellets containing the nuclear extract were then resuspended in 2% SDS lysis buffer (2% SDS, 10 mM Tris, pH 8.0, and 150 mM NaCl). 9 mg of spinal cord lysate was concentrated using 30,000-kDa-cutoff Millipore Centricon filters (EMD Millipore) and resolved by SDS-AGE. Western analysis was performed using AR(H280) (1:1000).

RESULTS

Intranuclear Inclusions in SBMA Cell Models Contain Full-length Androgen Receptor—We and others had previously reported that the intranuclear inclusions found within SBMA tissue and SBMA cell and animal models contain only N-terminal portions of the AR (4, 5, 7, 13, 14) as they are detected with antibodies directed against epitopes in the N-terminal region of the AR, such as AR(H280) and AR-318, but not with antibodies that detect AR epitopes in central or C-terminal regions of the AR, such as AR(441) and AR(C19) (Fig. 1*A*). To determine whether nuclear inclusions contain an N-terminal fragment or
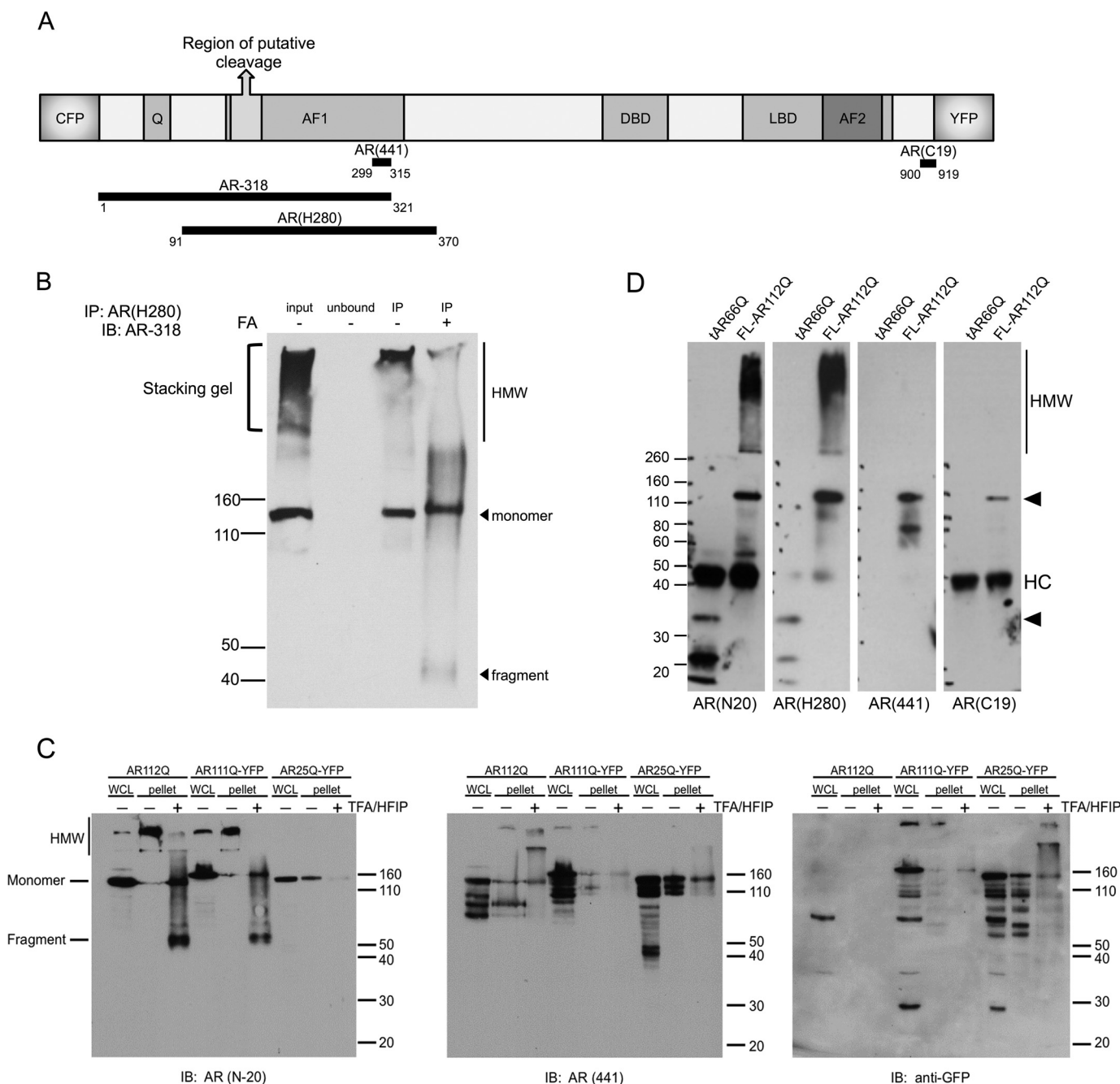
FIGURE 1. **High molecular weight AR species contain N-terminal, fragmented AR protein.** *A*, schematic representation of human AR protein domains: polyglutamine (*Q*), transactivation domains (*AF1* and *AF2*), DNA binding domain (*DBD*), ligand binding domain (*LBD*), and the putative region of cleavage that produces the N-terminal fragment. Epitopes to antibodies used in Western blotting, immunoprecipitation, and immunofluorescence detection are indicated as well as the orientation of fluorescent protein fusions. *B*, formic acid (*FA*) treatment of immunoprecipitated (*IP*) AR yields a ~45-kDa N-terminal AR fragment with concurrent loss of high molecular weight aggregated species (*HMW*) from the stacking gel. *C*, AR-containing insoluble aggregates from PC12 cells expressing AR112Q, AR111Q-YFP, or AR25Q-YFP were purified by ultracentrifugation and treated with TFA:HFIP. 25 μg of whole cell lysates (*WCL*) and a 250-μg equivalent of untreated or TFA:HFIP-treated samples were resolved by 10% SDS-PAGE and immunoblotted (*IB*) using anti-GFP antibody (to detect the C terminus of YFP-containing AR), then stripped and probed with AR(N-20) antibody (to detect N-terminal AR epitope), and then stripped and probed with AR(441) antibody (to detect the internal AR epitope). *D*, cell lysates from HEK293 cells transfected with tAR66Q and lysates from full-length AR112Q-expressing cell lines were immunoprecipitated with AR(H280). Immunopurified samples were resolved by SDS-PAGE and immunoblotted using antibodies AR(N-20), AR(H280), AR(441), and AR(C19). The *upper arrow* denotes full-length AR112Q, and the *lower arrow* denotes the migration of the tAR66Q. *HMW*, high molecular weight species in stacking gel; *HC*, IgG heavy chain resulting from immunoprecipitation.

fragments of the mutant AR, we either immunoprecipitated total AR (Fig. 1*B*) or sedimented insoluble AR (Fig. 1*C*) from protein extracts produced in PC12 cells that inducibly express the mutant AR either unlabeled (Fig. 1*B*) or tagged at the C terminus with YFP (Fig. 1*C*) and treated the precipitates with

either formic acid (Fig. 1*B*) or TFA:HFIP (Fig. 1*C*). The ~45-kDa AR fragment released by this treatment was detected with antibodies that detect the AR N terminus, AR(N-20) (Fig. 1*C*), AR-318 (Fig. 1*B*), and AR(H280) (not shown), but not with antibodies AR(441) and anti-GFP (Fig. 1*C*), similar to what was

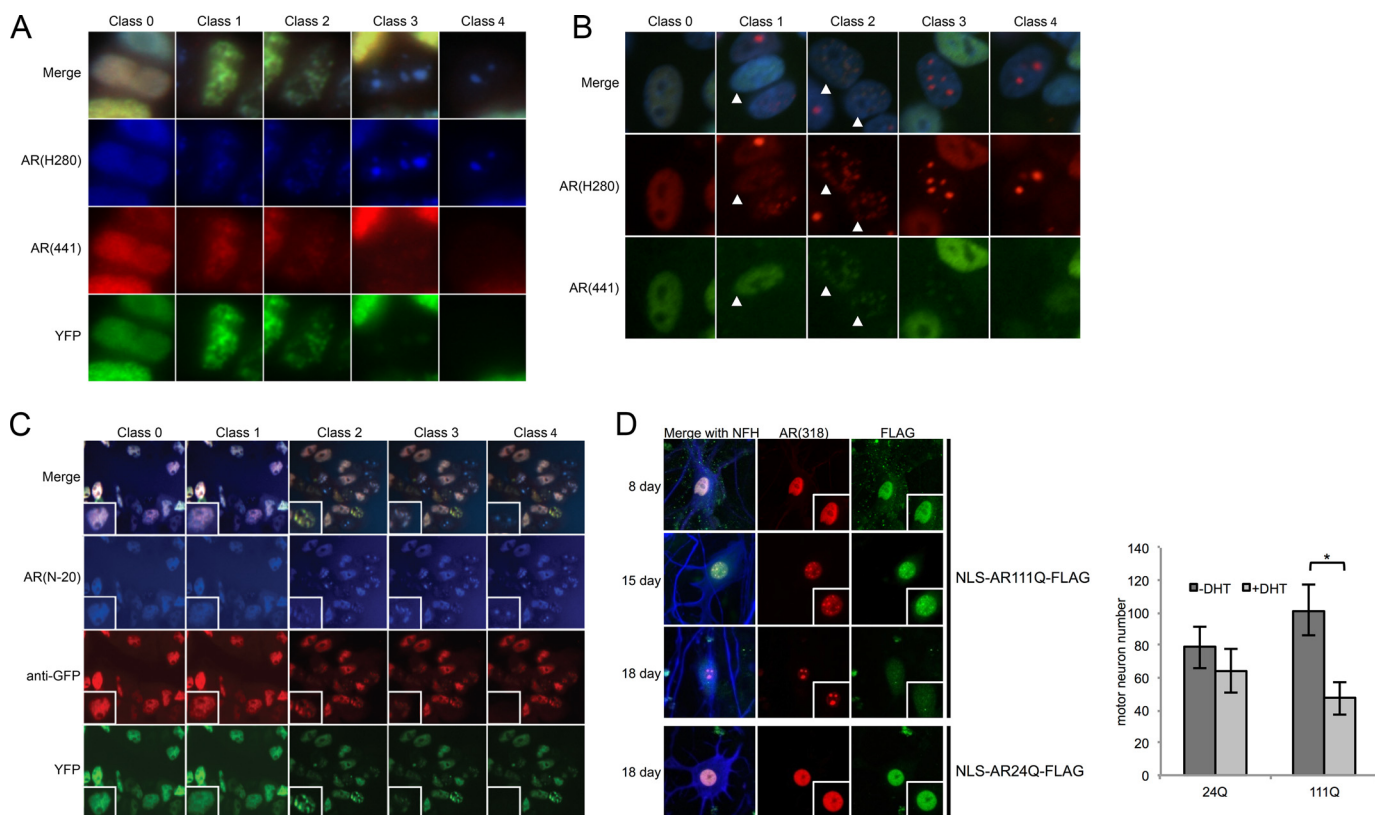# Proteolysis of Polyglutamine-expanded AR Is a Late Event

FIGURE 2. **PC12 cell models form inclusions containing full-length AR protein.** Classes 1–3 of inclusion-forming cells show the presence of the C terminus in inclusions, which are characterized by their size and nuclear abundance. *A*, DHT-treated PC12 cells expressing DLAR121Q immunostained with AR(H280); *green* fluorescence represents the YFP emission signal. Qualitative classification of aggregating cells was based on retention of the C terminus, inclusion size, and nuclear abundance. *B*, DHT-treated PC12 cells expressing AR112Q immunostained with AR(H280) and AR(441) to identify N and C epitopes, respectively. Qualitative classification of aggregating cells was based on the above criteria. *Arrowheads* indicate cells containing the indicated inclusion class. *Blue* fluorescence in the merge panels represents Hoechst staining to indicate nuclei. *C*, DHT-treated PC12 cells expressing AR111Q-YFP were immunostained with AR(N-20) and anti-GFP antibodies. *Green* fluorescence represents the YFP emission signal. *D*, dissociated spinal cord cultures from non-transgenic E13 mice were infected with AAV expressing FLAG-tagged human AR111Q or AR24Q and an exogenous NLS to ensure nuclear localization and treated with DHT for 3–18 days. Cells were immunostained using AR(H280) and anti-FLAG antibodies for detection of the N and C termini, respectively, and counterstained with SMI32 (anti-neurofilament heavy chain (*NFH*) antibody). Toxicity was evaluated by counting the number of motor neurons (based on morphology and SMI32 reactivity) from 10 random fields/coverslip with the observer blinded to the experimental conditions. Statistical analysis was evaluated using Student's *t* test (*, $p < 0.05$). Although a difference in motor neuron number is apparent between AR24Q- and AR111Q-expressing cultures, these differences are likely due to different inherent toxicities of the AAV preparations. Polyglutamine expansion-dependent toxicity was reproducibly observed. *Error bars* represent S.D.

previously observed with protein extracts from a transgenic mouse model of SBMA (14). To further understand the nature of the released fragment, we evaluated the immunoreactivity of the antibodies used here with an artificial fragment of the mutant AR that is truncated at amino acid 130 of the human AR (Fig. 1*D*). Expression of a polyglutamine-expanded form of this fragment in a variety of cultured cell types and in mice results in its aggregation and toxicity (18, 31, 32). For the experiments shown here, we expressed the truncated AR (tAR) with 66 glutamine repeats (tAR66Q) as expression of the 112-glutamine, truncated AR (tAR112Q) results in robust aggregation and little soluble AR. The tAR66Q migrated at ~35 kDa as expected, whereas soluble tAR112Q shown previously migrates at ~45 kDa (31), similar to the size of the formic acid- or TFA:HFIP-released AR fragment from nuclear inclusions formed upon full-length AR expression (Fig. 1, *B* and *C*). Immunoprecipitation with antibody AR(H280) followed by immunoblotting revealed that the AR fragment was detected by AR antibodies AR(N-20) and AR(H280) (Fig. 1*D*, *lower arrowhead*) but not by AR antibodies AR(441) and AR(C19), whereas all four antibodies detected full-length AR (Fig. 1*D*, *upper arrowhead*).

To further explore the timing and location of AR proteolysis, we created a PC12 cell model of SBMA that inducibly expresses full-length human AR with an expanded polyglutamine tract of 121 glutamines fused at the N and C termini with CFP and YFP, respectively (DLAR121Q). This cell model recapitulates the ligand- and polyglutamine length-dependent formation of intranuclear inclusions composed of labeled AR (Fig. 2*A* and data not shown) that is observed in PC12 cells expressing unlabeled AR (13). Although many of the nuclear inclusions lacked YFP fluorescence, some of the inclusions clearly contained YFP (Fig. 2*A*), indicating that at least a portion of the nuclear inclusions contained full-length, polyglutamine-expanded AR. From these observations, we broadly categorized the heterogeneous population of inclusion-containing cells into five classes based on the size and number of inclusions per nucleus as well as the relative proportion of N-terminal *versus* C-terminal fluorescence as determined by either CFP/YFP fluorescence, AR(H280) immunoreactivity/YFP fluorescence (Fig. 2*A*), or AR(H280)/AR(441) immunoreactivity (Fig. 2*B*). Specifically, Class 0 cells displayed a diffuse nuclear distribution of AR immunoreactivity. Class 1 cells showed a mottled appearance,

representing a change from the diffuse distribution of AR in Class 0 cells; both N-terminal and C-terminal antibody immunoreactivities were apparent. Class 2 cells displayed discrete puncta slightly reduced in number and larger in size than those of Class 1 cells. Both N-terminal and C-terminal antibody immunoreactivities were present, although the C-terminal signal was reduced. Class 3 cells displayed several large nuclear inclusions. In these inclusions, N-terminal antibody immunoreactivity was very strong, and C-terminal antibody immunoreactivity was present but very weak. Class 4 cells contained a small number of large nuclear inclusions detected only with N-terminal AR antibodies.

To further explore the idea that inclusions contain full-length AR and to ensure that this observation was not an artifact of the fusion protein, we treated PC12 cells expressing AR112Q with DHT and immunostained the cells to determine the presence or absence of the internal AR epitope (AR(441)) in nuclear inclusions identified by the presence of the N-terminal epitope (AR(H280)). A population of AR-containing intranuclear inclusions was also detected by AR(441) (Fig. 2B), indicating that the epitope downstream of the putative cleavage point was present in some inclusions but absent from others. Antibodies detecting the extreme C terminus of the AR perform poorly in immunostaining protocols. Therefore, to further determine the retention of the C terminus in the inclusions described as Classes 1, 2, and 3 (Fig. 2, A and B), we created stable, inducible cell lines expressing full-length AR111Q fused with YFP at the C terminus. Following induction of AR expression with doxycycline and treatment with DHT, cells were immunostained with antibodies to the extreme N terminus (AR(N-20)) and the extreme C terminus (anti-GFP). The inherent YFP fluorescence was also observed as a marker for the C terminus of the AR. Results of these experiments reveal the same immunoreactivity of AR inclusion classes shown in Fig. 2, A and B, using antibodies AR(N-20) and anti-GFP (Fig. 2C), further supporting the idea that some inclusion classes (1, 2, and 3) contain full-length AR, whereas others (Class 4) do not.

To evaluate our findings in a disease-relevant model, we analyzed nuclear inclusions in primary motor neurons expressing the mutant, polyglutamine-expanded AR. Dissociated spinal cord cultures from wild-type mice were differentiated for 3 weeks and then infected with AAV to express full-length human AR (AR24Q or AR111Q) tagged with a C-terminal FLAG epitope. As previously shown for motor neurons expressing untagged polyglutamine-expanded AR (27, 29, 30), a substantial number of motor neurons died by 8 days of treatment with DHT (Fig. 2D, *right panel*). We did not detect the formation of nuclear inclusions in motor neurons during this time (Fig. 2D, *left panel*). However, treatment of cultures expressing AR111Q, but not AR24Q, for 11 days or longer resulted in the formation of small nuclear inclusions within motor neurons; these NI were detected with antibodies to both N-terminal (AR(H280)) and C-terminal (FLAG) epitopes (Fig. 2D, *15 day panel*), revealing the presence of full-length AR in inclusions. Continued DHT treatment (18 days) resulted in the formation of larger inclusions, many of which lacked immunoreactivity with the C-terminal antibody (FLAG) (Fig. 2D, *18 day panel*), consistent with the loss of the C terminus and revealing
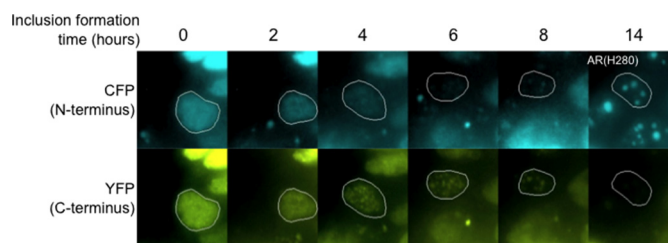

FIGURE 3. **Live cell imaging reveals that polyglutamine-expanded AR forms nuclear inclusions prior to cleavage.** CFP and YFP fluorescence images of DHT-treated PC12 DLAR121Q-expressing cells were taken every 2 h for 20 h. After the final time point, cells were fixed and immunostained using AR(H280), and a final series of images was taken. The *circled* cell highlights a single representative inclusion-forming cell over time.

its occurrence as a late event in motor neurons. Motor neurons expressing AR24Q-FLAG did not form nuclear inclusions or die in response to DHT treatment (Fig. 2D).

Inclusion Populations Represent Temporal Stages in an Aggregation Continuum—We next sought to determine whether the observed inclusion classes represent discontinuous populations of nuclear inclusions or whether they are part of an aggregation continuum. Utilizing the double labeled DLAR121Q-expressing cell line, we performed live cell imaging to track the AR N and C termini within inclusions over time. DLAR121Q-expressing PC12 cells were treated with DHT for 72 h prior to live cell imaging and for an additional 24 h during imaging. To observe the presence of the AR N terminus (CFP) and C terminus (YFP), we captured CFP and YFP images every 2 h for 24 h. After image collection, the cells were immunostained to identify the N terminus of the AR, and a final image was taken. In some experiments, immunostaining of the internal AR epitope (using antibody AR(441)) was carried out. Time lapse images of cells with inclusions revealed the formation of small, Class 1 puncta containing CFP- and YFP-positive AR in cells with previously diffuse, nuclear, full-length AR (Fig. 3). With time, these puncta became larger and fewer in number and progressively lost the YFP signal but maintained the CFP signal. The final immunodetection of the AR N terminus verified its presence despite a weak CFP signal. We validated the loss of the AR C terminus by immunostaining live imaged cells with antibody AR(441) (not shown). This result confirms our interpretation that inclusions lacking the YFP signal also lack epitopes downstream of the putative cleavage site, substantiating the use of YFP as a marker for the AR C terminus in these live imaging experiments. These data support the conclusion that inclusions form through the aggregation of full-length polyglutamine-expanded AR protein, which is subsequently cleaved within nuclear inclusions.

The observation that the distinct inclusion classes observed here represent a continuum of inclusion formation and maturation allowed us to evaluate the consistency of the timing of this process. Using the data acquired from live cell imaging, we found that, despite the stochastic nature of cellular inclusion formation, nuclear AR transitions from early Class 1 puncta containing full-length AR protein to large intranuclear inclusions composed of completely cleaved AR protein in a consistent time frame averaging 8.4 h (range, 4–12 h). This finding suggests that the visible maturation of inclusions from their

initial formation to their loss of C-terminal epitopes is a uniform process.

Soluble and Insoluble Aggregation Species Contain Full-length AR—The finding that nuclear inclusions form from full-length polyglutamine-expanded AR predicts that soluble, preinclusion AR aggregation species are also composed of full-length AR. To evaluate this prediction, we utilized SDS-AGE, which was previously shown to be a sensitive and specific method for resolving polyglutamine-expanded aggregates (23, 24, 33). Using SDS-AGE, we detected a heterogeneous population of AR species that are both polyglutamine length-dependent and hormone-dependent (Fig. 4*A*). Moreover, two distinct populations of AR species with differing migration patterns were observed (Fig. 4*A*). Slow migrating AR species formed within 2 h of hormone treatment; with continued hormone treatment, faster migrating species appeared that were temporally correlated with the appearance of cytologically detectable nuclear inclusions (Fig. 4*A*, *right*). Additionally, we discovered that both slow and fast migrating species contain full-length AR as revealed by their detection with N-terminal antibodies AR(N-20) and AR(H280) and with C-terminal antibodies AR(441) and AR(C19) (Fig. 4, *A* and *B*).

To develop a more detailed biochemical understanding of SDS-AGE-resolvable AR species, we carried out assays to determine the sedimentation characteristics of slow and fast migrating polyglutamine-expanded AR species. Using ultracentrifugation, we found that slow migrating AR species are SDS-soluble, whereas fast migrating AR species are largely SDS-insoluble (Fig. 4*C*). Moreover, as expected from experiments using whole-cell lysates (Fig. 4*A*), both SDS-soluble and SDS-insoluble species contain full-length AR (Fig. 4*C*). These data support the idea that full-length AR forms soluble aggregation species within a few hours of hormone binding. At later times, when nuclear inclusions are formed, full-length AR is found within insoluble aggregates.

The C Terminus Is Lost from Fast Migrating SDS-AGE Species—Our observation that the loss of C-terminal epitopes from AR inclusions is a late event (Fig. 3) prompted us to evaluate the loss of C-terminal epitopes from SDS-AGE-resolvable AR species. To do this, we induced the formation of untagged or YFP-tagged AR aggregates in PC12 cells with doxycycline and DHT. After 5 days of induction, we prevented further AR synthesis by removing doxycycline and followed the fate of AR N- and C-terminal epitopes using SDS-AGE. We observed the loss of AR(441) immunoreactivity from fast migrating AR species (Fig. 4*D*); this loss correlated with the decrease in AR(441)-positive nuclear inclusions (Fig. 4*D*, *right*). Moreover, in protein extracts from cells expressing AR tagged with YFP at the C terminus, we observed the loss of YFP from fast migrating species after doxycycline washout (Fig. 5, *F* and *G*). Thus, our observations that 1) both slow and fast migrating species detected by SDS-AGE contain full-length AR and 2) internal (AR(441)) and C-terminal (YFP) immunoreactivities are lost from late, fast migrating, but not from early, slow migrating, species support the idea that AR cleavage to form an aberrant fragment is a late event.

Fast Migrating Species Contain Ubiquitin—Previous studies have shown the presence of ubiquitin and other proteasomal components associated with inclusions of polyglutamine-expanded AR in models of SBMA (7, 13, 18, 34, 35). If the fast migrating species represent inclusions or an inclusion-associated aggregation species, we would expect these species to be ubiquitinated. Indeed, Western analysis using an anti-ubiquitin antibody revealed that fast migrating, but not slow migrating, species are immunoreactive for ubiquitin (Fig. 5*A*).

Proteasome Inhibition Prevents AR Processing within NI—The importance of the ubiquitin-proteasome system in polyglutamine protein aggregation and inclusion formation has been described (36–38), prompting us to evaluate the role of the proteasome in AR proteolysis. In PC12 cells inducibly expressing polyglutamine-expanded AR, inhibition of the proteasome with epoxomicin reduced the percentage of inclusions containing cleaved AR in a dose-dependent manner without altering the overall inclusion load (Fig. 5*B*), suggesting a role for the proteasome in AR proteolysis within maturing NI.

Proteasome Inhibition Prevents AR Proteolysis within Fast Migrating Species—Our finding that proteasome inhibition altered the state of AR proteolysis within nuclear inclusions (Fig. 5*B*) and that fast migrating aggregation species contain ubiquitin (Fig. 5*A*) prompted us to evaluate the effect of proteasome inhibition on the loss of C-terminal epitopes within SDS-AGE-identified AR aggregation species. SDS-AGE analysis of untagged (Fig. 5*C*) or YFP-tagged (Fig. 5*F*) AR species from cells induced for 5 days to form inclusions and then treated with or without epoxomicin in the absence of new AR protein synthesis showed a marked retention of AR(441) and YFP epitopes in fast migrating species when treated with epoxomicin (Fig. 5, *C*, *D*, and *F*; in *C* and *F*, *right panels*, compare *lanes 9–12* with *lanes 5–8*), correlating with the retention of full-length AR in nuclear inclusions upon proteasome inhibition (Fig. 5, *E* and *G*). These data support the idea that the proteasome is involved in cleavage of the AR following its incorporation into insoluble aggregates.

A polyglutamine-specific antibody detects soluble, full-length, expanded AR—Identification of distinct aggregation species in SBMA and other polyglutamine repeat diseases is important for understanding both disease mechanisms and targets for therapeutic intervention. 3B5H10, a polyglutamine-specific antibody that detects a compact, hairpin structure of polyglutamine (39), predicts toxicity in a Huntington disease cell model (22) and thus likely detects a toxic species of other expanded polyglutamine proteins. Moreover, 3B5H10 detects expanded, but not normal, forms of AR by Western blot analysis (22), although a recent study indicates that, like two other polyglutamine-specific antibodies (1C2 and MW1), 3B5H10 can detect normal length polyglutamine tracts (40). Here we show that inclusions that are visible by light microscopy failed to be detected by 3B5H10 (Fig. 6, *A* and *B*); even the most immature Class 1 puncta failed to be detected with 3B5H10. This finding suggests that, once incorporated into inclusions, the 3B5H10 epitope is sequestered. Based on our observations from SDS-AGE that slow migrating AR species are soluble, we hypothesized that these species would be immunoreactive with 3B5H10. Indeed, slow migrating, but not fast migrating, AR species present an epitope that bound 3B5H10 (Fig. 6*C*). Together, these findings
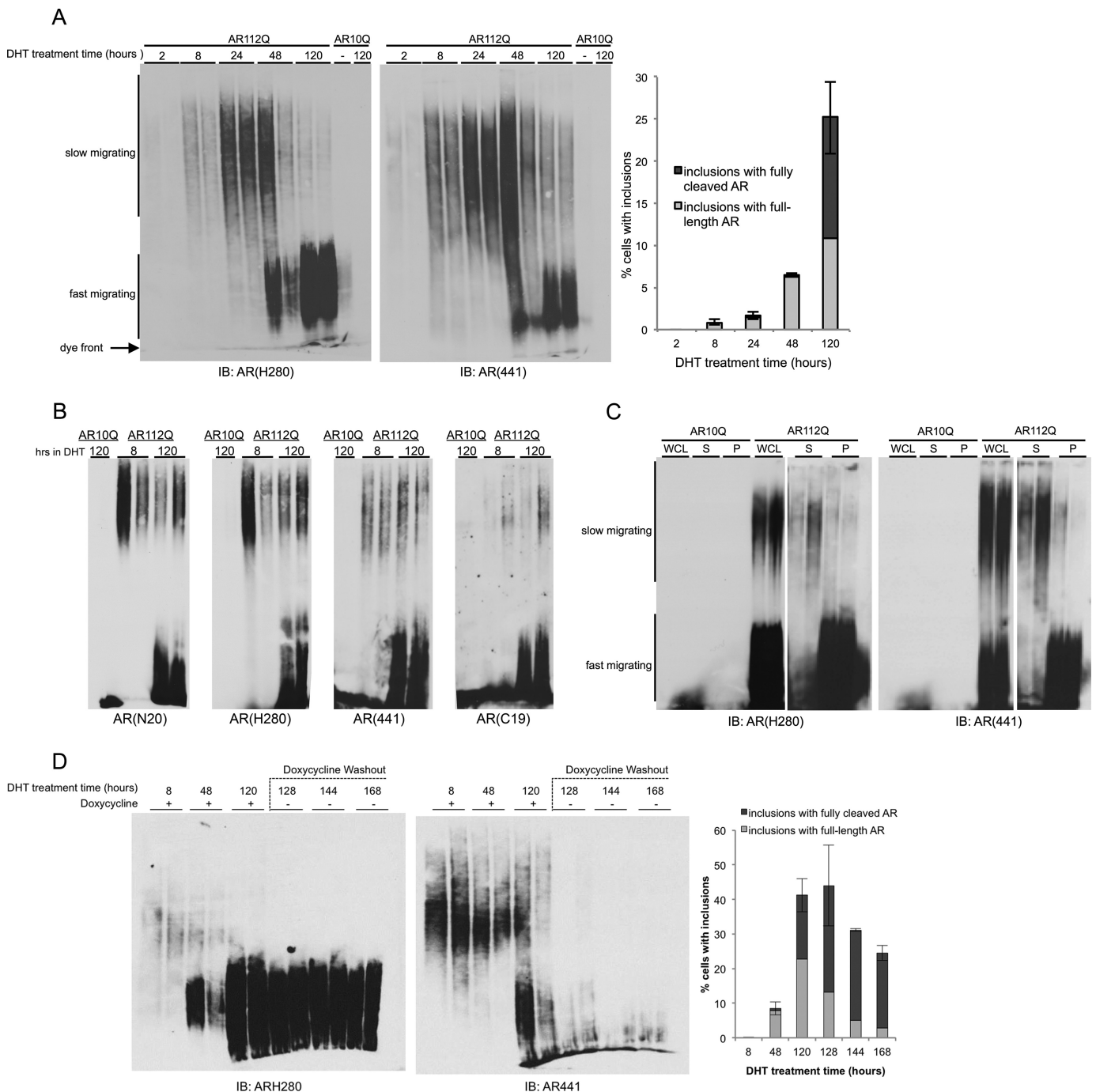
FIGURE 4. **Distinct slow and fast migrating aggregation species are formed by polyglutamine-expanded AR, contain full-length AR protein, and are proteolyzed with time.** *A*, lysates of DHT-treated PC12 cells expressing AR112Q or AR10Q were resolved using 1% SDS-agarose gel electrophoresis. Total AR and full-length AR were detected using AR(H280) and AR(441), respectively. Slow and fast migrating AR species (indicated) form in a polyglutamine length- and hormone-dependent manner and contain full-length AR protein (AR(441) immunoreactivity); fast migrating species correlate with inclusion load as determined by immunofluorescence imaging (*right* graph). *Error bars* represent S.D. *B*, PC12 cells were induced with doxycycline to express AR112Q or AR10Q and treated with DHT for 8 or 120 h. Protein lysates were resolved using 1% SDS-AGE; Western analysis was performed with AR(441) and AR(C19) followed by AR(H280) and AR(N-20). *C*, fast migrating species of AR112Q are pelleted by ultracentrifugation; slow migrating species remain soluble. Both species contain full-length AR. *S*, supernatant; *P*, pellet; *WCL*, whole-cell lysate. The *right side* of each panel represents a darker exposure than the *left side* to reveal the fainter slow migrating species. Western analysis for GAPDH was performed to control for soluble contaminant in the insoluble fraction (not shown). *D, left*, PC12 cells were induced with doxycycline to express AR112Q and treated with DHT for 8, 48, or 120 h. After 120 h, expression of new protein was stopped by withdrawal of doxycycline, but DHT treatment continued for an additional 8, 24 or 48 h. Protein lysates were resolved using 1% SDS-AGE, Western analysis was performed with AR(441), and then blots were stripped and probed for AR(H280) to show the loss of C-terminal epitopes over time. *Right*, cells treated in *A* were immunostained for AR(H280) and AR(441), and cells containing AR(441)-positive and AR(441)-negative inclusions were quantified. *IB*, immunoblotting.
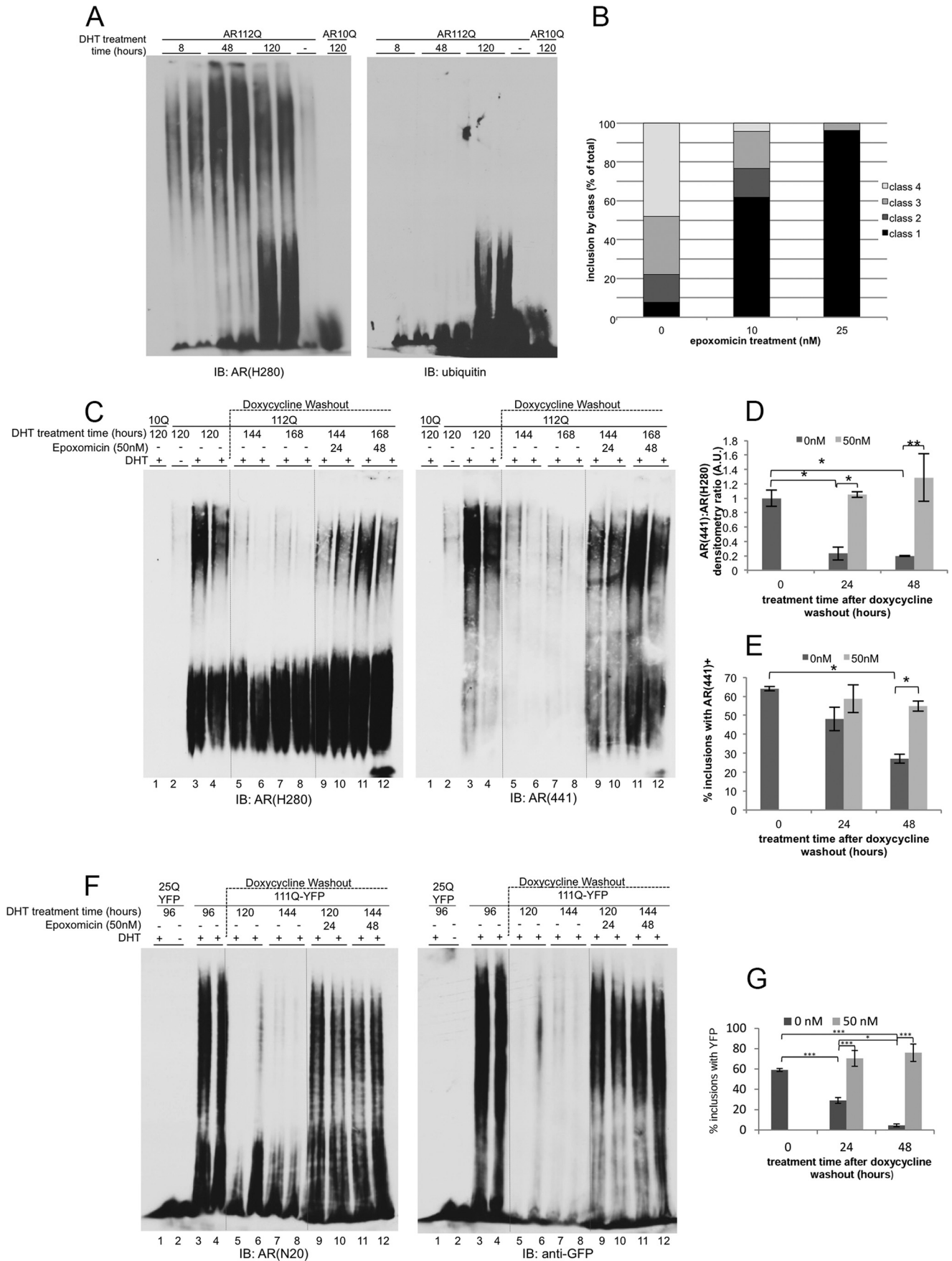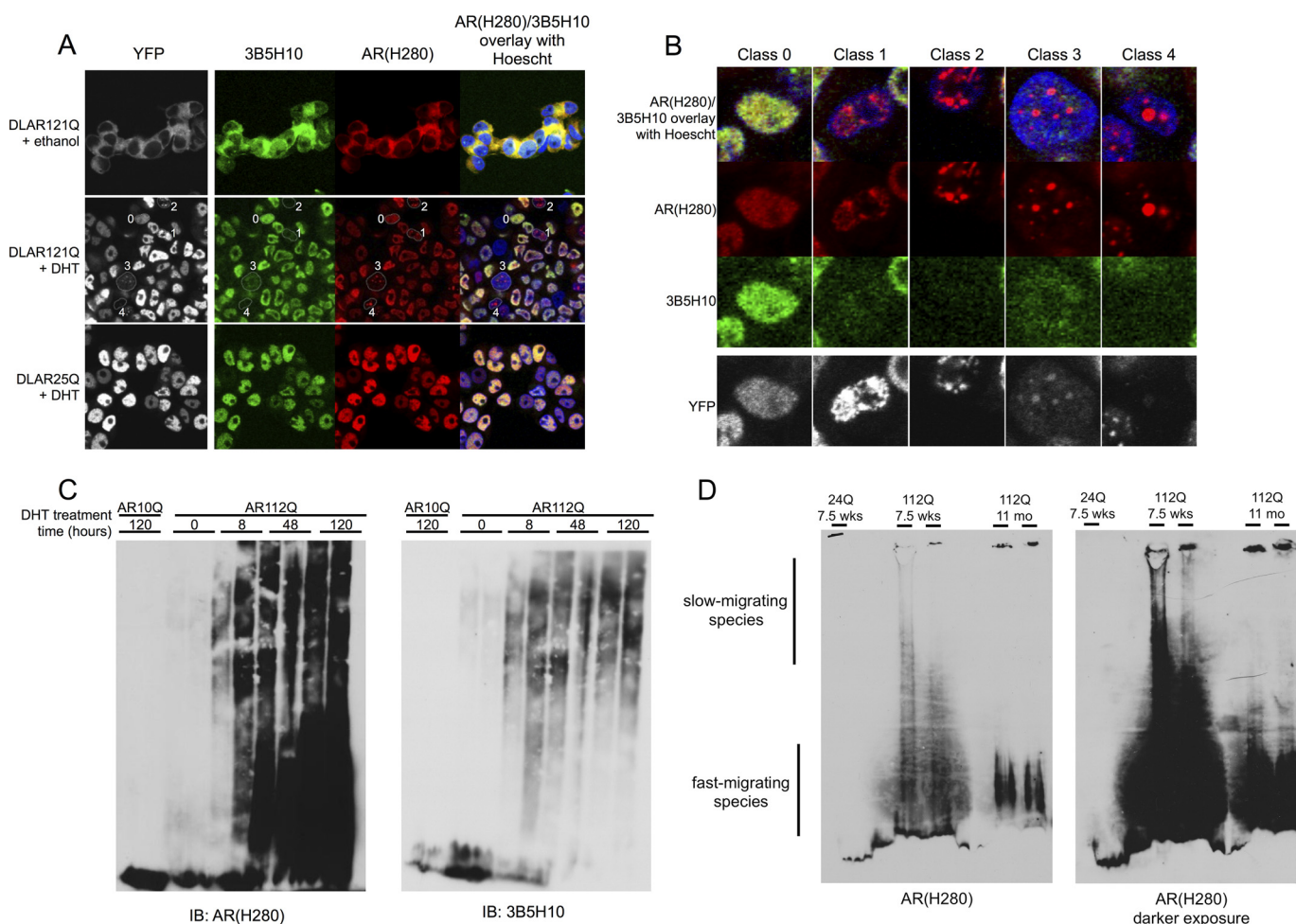
FIGURE 6. **AR inclusions and fast migrating species fail to be detected with the polyglutamine-specific antibody 3B5H10.** *A* and *B*, DHT-treated PC12 cells expressing DLAR121Q or DLAR25Q were immunostained with AR(H280) and 3B5H10. The overlay shows that cells with inclusions are not detected with 3B5H10. YFP fluorescence enables classification of inclusions by identifying full-length AR. Cells in each of the five classifications have been *circled* and labeled in *A* and enlarged in *B*. *C*, lysates of DHT-treated PC12 cells expressing AR112Q or AR10Q were resolved using 1% SDS-agarose gel electrophoresis and detected by Western blot with 3B5H10 followed by AR(H280) after stripping. 3B5H10 fails to detect fast migrating but does detect slow migrating AR species. *D*, spinal cord nuclear extracts from male PrPAR112Q transgenic mice display slow and fast migrating aggregation species. Each lane represents nuclear extracts from two pooled spinal cords. Slow migrating species are detected as early as 7.5 weeks at an age that precedes the formation of large nuclear inclusions. The *right panel* is a long exposure to reveal the presence of slow migrating species in both 7.5-week samples and their absence from 11-month samples. *IB*, immunoblotting.

indicate that slow migrating AR species comprise full-length, soluble, and 3B5H10-reactive AR aggregates.

We next investigated whether slow migrating species could be detected *in vivo*. To this end, we performed nuclear fractionation from spinal cords of both presymptomatic (7.5-week-old) and symptomatic (11-month-old) male transgenic mice expressing human AR with an expanded (AR112Q) polyglutamine tract (7). Although we detected both slow and fast migrating species in spinal cords of 7.5-week-old transgenic

male SBMA mice, 11-month-old male transgenic mice exhibited only fast migrating species (Fig. 6*D*), consistent with the presence of abundant, prominent nuclear inclusions at this age as described previously (7). Small cytologically detectable puncta can already be observed by 6 weeks of age (7), likely explaining the observation of some fast migrating species at 7.5 weeks. The appearance of slow migrating species prior to the detection of motor deficits further supports the idea that these aggregation species correlate with toxicity both *in vitro* and *in vivo*.

FIGURE 5. **Insoluble, fast migrating AR aggregation species contain full-length AR and ubiquitin and become proteolyzed over time in a proteasome-dependent manner.** *A*, lysates from DHT-treated cells expressing AR112Q or AR10Q were resolved by 1% SDS-agarose gel electrophoresis. A Western blot using antibodies against AR (AR(H280)) and ubiquitin shows that only fast migrating AR species are detectable with an anti-ubiquitin antibody. *B*, PC12 cells expressing DLAR121Q were treated simultaneously with epoxomicin and DHT for 48 h. The increasing epoxomicin dose resulted in an increased population of inclusions that retained the AR C terminus (full length) without a change in overall inclusion load as detected with AR(H280). *C* and *F*, PC12 cells expressing AR112Q or AR10Q (*C*) or AR111Q-YFP or AR25Q-YFP (*F*) were treated with DHT for the indicated time. Expression of new protein was stopped by withdrawal of doxycycline, but DHT treatment continued for an additional 24 or 48 h in the presence or absence of epoxomicin. Protein lysates were resolved using 1% SDS-AGE. Western analysis using AR(441) (*C*) or anti-GFP (*F*) and AR(H280) (*C*) or AR(N-20) (*F*) show the loss of AR(441) (*C*) and GFP (*F*) epitopes over time in the absence of epoxomicin and their retention in the presence of epoxomicin. *D* and *G*, quantification of signal intensities in *C* and *F*, respectively, using ImageJ (*, $p < 0.05$; **, $p < 0.001$). *Error bars* represent S.D. *E*, cells treated in *C* were immunostained for AR(H280) and AR(441), and cells containing inclusions detected by both antibodies were quantified (*, $p < 0.05$). *Error bars* represent S.D. Statistical analysis was carried out using two-way analysis of variance with post hoc Tukey test (SigmaStat). *IB*, immunoblotting; *A.U.*, absorbance units.

DISCUSSION

The presence of cleaved, polyglutamine-expanded androgen receptor protein in intranuclear inclusions of patient tissue and disease models of SBMA previously suggested the relevance of this cleavage in the disease process. In addition, observations that expression of a truncated AR results in substantially greater toxicity (18, 31, 41) than does expression of the full-length expanded polyglutamine protein (7, 11, 29) suggested that proteolysis of the polyglutamine-expanded AR produces a toxic and aggregation-prone fragment. We therefore sought to explore the mechanism and timing of AR cleavage. Here we have shown that, contrary to our expectations, AR inclusions were formed from full-length androgen receptor, and cleavage of the AR occurred within maturing inclusions. Maturation of inclusions in this system occurred within a consistent time frame, suggesting that once the mutant AR forms cytologically detectable Class 1 inclusions an intrinsic property of the system exists to facilitate or promote the formation of fully proteolyzed Class 4 inclusions. A role for the proteasome in this process is supported by our data.

A previous report that soluble oligomers comprise AR fragments (14) led us to reevaluate the presence of full-length polyglutamine-expanded AR in soluble, preinclusion AR species. To further understand the biochemical characteristics of AR aggregation species, we utilized SDS-AGE, a highly sensitive and specific method to evaluate polyglutamine-expanded aggregated species (23, 24, 33). We demonstrate the formation of two distinct, albeit heterogeneous, aggregation species resolved by SDS-AGE and show that early, soluble aggregation species consist of full-length AR, whereas the insoluble AR aggregation species that are formed at later time points comprise both full-length and proteolyzed AR. Moreover, the formation of insoluble, fast migrating AR aggregation species is tightly correlated with the appearance of cytologically detectable inclusions, suggesting that fast migrating SDS-AGE species represent either the biochemical correlate of nuclear inclusions or an inclusion-associated, insoluble aggregation species. Further support for this interpretation comes from our finding that C-terminal AR epitopes were lost from both mature nuclear inclusions and fast migrating SDS-AGE species. The differences between our observations described here and those described by Li *et al.* (14) likely result both from the different sedimentation conditions used and the high sensitivity of the SDS-AGE analysis used here. Whether the oligomeric AR species described using atomic force microscopy in the Li *et al.* (14) study represent one of the aggregated AR species described here will be the subject of future studies.

The observation that fast migrating AR aggregation species correlated with the appearance of large, cytologically detectable nuclear inclusions and were sedimented upon ultracentrifugation whereas slow migrating AR species appeared prior to fast migrating species and were soluble upon ultracentrifugation is at first glance counterintuitive because one would assume that slower migrating species would be larger and likely correlate with cytologically visible inclusions. However, the sieving nature of agarose retards molecules with extended conformations and allows more compacted molecules to migrate faster in a common electrical field. Thus, we hypothesize that SDS-AGE-resolvable slow migrating AR species are characterized by an extended conformation with a lower molecular weight than the more compact fast migrating AR species. These characteristics may inform future work on the nature of these species as the heterogeneity within each of these populations is yet to be defined.

There have been many studies focused on defining the protease responsible for cleaving the polyglutamine-expanded AR. Earlier studies revealed a role for caspase-3 cleavage in the production of a toxic AR fragment (42) in a system in which hormone binding to the mutant AR prevented, rather than caused, its cleavage and toxicity. In our present studies, we found that proteasome activity was required for the loss of AR C-terminal epitopes within inclusions as well as within fast migrating SDS-AGE-resolved AR aggregation species. The presence of ubiquitin in fast migrating SDS-AGE-resolved AR aggregation species as well as the loss of a detectable C-terminal fragment supports the idea that the proteasome mediates the cleavage of polyglutamine-expanded AR via the processive proteolysis of the AR from a C- to N-terminal direction. Previous studies have demonstrated the presence of proteasomes within polyglutamine-containing inclusions; however, whether such proteasomes are functional had not been defined. A recent study (43) provides evidence for active proteasomes within polyglutamine inclusions, supporting the idea that proteasomal processing of the polyglutamine-expanded AR can occur within maturing nuclear inclusions.

Identifying the protein species and associated mechanisms responsible for toxicity is one of the greatest challenges within the polyglutamine disease field, and the development and characterization of polyglutamine-specific antibodies have the potential to address this challenge. A recently identified expanded polyglutamine-specific antibody, 3B5H10, predicts risk of death in cell models of Huntington disease (22). Whether such findings hold for SBMA is currently unknown. Nonetheless, there is substantial support for the idea that soluble, preinclusion aggregation species form the basis of neuronal toxicity. Our studies using this antibody revealed that 3B5H10 failed to detect all nuclear inclusions regardless of class, suggesting that the epitope is rapidly sequestered within developing inclusions. The detection of SDS-AGE-resolvable slow migrating AR species with 3B5H10 suggests that the toxic AR species is likely found within this population of full-length AR. Ongoing studies are designed to further characterize these species. Our finding that AR proteolysis occurred after the formation of 3B5H10-reactive species strongly suggests that proteolysis is unrelated to toxicity. Although AR fragments that mimic the size of the proteolyzed species are highly toxic and aggregation-prone (18, 31, 41), our data reveal that such species are not the primary cause of toxicity in the context of full-length polyglutamine-expanded AR expression. Thus, our data show that, in cell models of SBMA, the detectable loss of the AR C terminus is a late event preceded by the formation of soluble AR aggregation species and cytological inclusions. Our findings thus reclassify the view of polyglutamine-expanded AR toxicity in SBMA and focus attention toward a mechanistic understanding of

upstream events impacting the conversion of full-length AR to a toxic species.

Note Added in Proof—Lori Zboray's contributions to this article fulfill the JBC authorship criteria, but her authorship was inadvertently omitted from the version of the article that was published on March 20, 2015 as a Paper in Press.

REFERENCES

1. Kennedy, W. R., Alter, M., and Sung, J. H. (1968) Progressive proximal spinal and bulbar muscular atrophy of late onset: a sex-linked recessive trait. *Neurology* **18,** 671–680
2. La Spada, A. R., Wilson, E. M., Lubahn, D. B., Harding, A. E., and Fischbeck, K. H. (1991) Androgen receptor gene mutations in X-linked spinal and bulbar muscular atrophy. *Nature* **352,** 77–79
3. Sobue, G., Hashizume, Y., Mukai, E., Hirayama, M., Mitsuma, T., and Takahashi, A. (1989) X-linked recessive bulbospinal neuronopathy: a clinicopathological study. *Brain* **112,** 209–232
4. Li, M., Miwa, S., Kobayashi, Y., Merry, D. E., Yamamoto, M., Tanaka, F., Doyu, M., Hashizume, Y., Fischbeck, K. H., and Sobue, G. (1998) Nuclear inclusions of the androgen receptor protein in spinal and bulbar muscular atrophy. *Ann. Neurol.* **44,** 249–254
5. Li, M., Nakagomi, Y., Kobayashi, Y., Merry, D. E., Tanaka, F., Doyu, M., Mitsuma, T., Hashizume, Y., Fischbeck, K. H., and Sobue, G. (1998) Nonneural nuclear inclusions of androgen receptor protein in spinal and bulbar muscular atrophy. *Am. J. Pathol.* **153,** 695–701
6. Orr, H. T., and Zoghbi, H. Y. (2007) Trinucleotide repeat disorders. *Annu. Rev. Neurosci.* **30,** 575–621
7. Chevalier-Larsen, E. S., O'Brien, C. J., Wang, H., Jenkins, S. C., Holder, L., Lieberman, A. P., and Merry, D. E. (2004) Castration restores function and neurofilament alterations of aged symptomatic males in a transgenic mouse model of spinal and bulbar muscular atrophy. *J. Neurosci.* **24,** 4778–4786
8. Katsuno, M., Adachi, H., Kume, A., Li, M., Nakagomi, Y., Niwa, H., Sang, C., Kobayashi, Y., Doyu, M., and Sobue, G. (2002) Testosterone reduction prevents phenotypic expression in a transgenic mouse model of spinal and bulbar muscular atrophy. *Neuron* **35,** 843–854
9. Takeyama, K., Ito, S., Yamamoto, A., Tanimoto, H., Furutani, T., Kanuka, H., Miura, M., Tabata, T., and Kato, S. (2002) Androgen-dependent neurodegeneration by polyglutamine-expanded human androgen receptor in *Drosophila. Neuron* **35,** 855–864
10. Yu, Z., Dadgar, N., Albertelli, M., Gruis, K., Jordan, C., Robins, D. M., and Lieberman, A. P. (2006) Androgen-dependent pathology demonstrates myopathic contribution to the Kennedy disease phenotype in a mouse knock-in model. *J. Clin. Investig.* **116,** 2663–2672
11. Montie, H. L., Cho, M. S., Holder, L., Liu, Y., Tsvetkov, A. S., Finkbeiner, S., and Merry, D. E. (2009) Cytoplasmic retention of polyglutamine-expanded androgen receptor ameliorates disease via autophagy in a mouse model of spinal and bulbar muscular atrophy. *Hum. Mol. Genet.* **18,** 1937–1950
12. Nedelsky, N. B., Pennuto, M., Smith, R. B., Palazzolo, I., Moore, J., Nie, Z., Neale, G., and Taylor, J. P. (2010) Native functions of the androgen receptor are essential to pathogenesis in a *Drosophila* model of spinal and bul-bar muscular atrophy. *Neuron* **67,** 936–952
13. Walcott, J. L., and Merry, D. E. (2002) Ligand promotes intranuclear inclusions in a novel cell model of spinal and bulbar muscular atrophy. *J. Biol. Chem.* **277,** 50855–50859
14. Li, M., Chevalier-Larsen, E. S., Merry, D. E., and Diamond, M. I. (2007) Soluble androgen receptor oligomers underlie pathology in a mouse model of spinobulbar muscular atrophy. *J. Biol. Chem.* **282,** 3157–3164
15. DiFiglia, M., Sapp, E., Chase, K. O., Davies, S. W., Bates, G. P., Vonsattel, J. P., and Aronin, N. (1997) Aggregation of huntingtin in neuronal intranuclear inclusions and dystrophic neurites in brain. *Science* **277,** 1990–1993
16. Hodgson, J. G., Agopyan, N., Gutekunst, C. A., Leavitt, B. R., LePiane, F., Singaraja, R., Smith, D. J., Bissada, N., McCutcheon, K., Nasir, J., Jamot, L., Li, X. J., Stevens, M. E., Rosemond, E., Roder, J. C., Phillips, A. G., Rubin, E. M., Hersch, S. M., and Hayden, M. R. (1999) A YAC mouse model for Huntington's disease with full-length mutant huntingtin, cytoplasmic toxicity, and selective striatal neurodegeneration. *Neuron* **23,** 181–192
17. Schilling, G., Wood, J. D., Duan, K., Slunt, H. H., Gonzales, V., Yamada, M., Cooper, J. K., Margolis, R. L., Jenkins, N. A., Copeland, N. G., Takahashi, H., Tsuji, S., Price, D. L., Borchelt, D. R., and Ross, C. A. (1999) Nuclear accumulation of truncated atrophin-1 fragments in a transgenic mouse model of DRPLA. *Neuron* **24,** 275–286
18. Abel, A., Walcott, J., Woods, J., Duda, J., and Merry, D. E. (2001) Expression of expanded repeat androgen receptor produces neurologic disease in transgenic mice. *Hum. Mol. Genet.* **10,** 107–116
19. Arrasate, M., Mitra, S., Schweitzer, E. S., Segal, M. R., and Finkbeiner, S. (2004) Inclusion body formation reduces levels of mutant huntingtin and the risk of neuronal death. *Nature* **431,** 805–810
20. Saudou, F., Finkbeiner, S., Devys, D., and Greenberg, M. E. (1998) Huntingtin acts in the nucleus to induce apoptosis but death does not correlate with the formation of intranuclear inclusions. *Cell* **95,** 55–66
21. Simeoni, S., Mancini, M. A., Stenoien, D. L., Marcelli, M., Weigel, N. L., Zanisi, M., Martini, L., and Poletti, A. (2000) Motoneuronal cell death is not correlated with aggregate formation of androgen receptors containing an elongated polyglutamine tract. *Hum. Mol. Genet.* **9,** 133–144
22. Miller, J., Arrasate, M., Brooks, E., Libeu, C. P., Legleiter, J., Hatters, D., Curtis, J., Cheung, K., Krishnan, P., Mitra, S., Widjaja, K., Shaby, B. A., Lotz, G. P., Newhouse, Y., Mitchell, E. J., Osmand, A., Gray, M., Thulasiramin, V., Saudou, F., Segal, M., Yang, X. W., Masliah, E., Thompson, L. M., Muchowski, P. J., Weisgraber, K. H., and Finkbeiner, S. (2011) Identifying polyglutamine protein species *in situ* that best predict neurodegeneration. *Nat. Chem. Biol.* **7,** 925–934
23. Sontag, E. M., Lotz, G. P., Agrawal, N., Tran, A., Aron, R., Yang, G., Necula, M., Lau, A., Finkbeiner, S., Glabe, C., Marsh, J. L., Muchowski, P. J., and Thompson, L. M. (2012) Methylene blue modulates huntingtin aggregation intermediates and is protective in Huntington's disease models. *J. Neurosci.* **32,** 11109–11119
24. Weiss, A., Klein, C., Woodman, B., Sathasivam, K., Bibel, M., Régulier, E., Bates, G. P., and Paganetti, P. (2008) Sensitive biochemical aggregate detection reveals aggregation onset before symptom development in cellular and murine models of Huntington's disease. *J. Neurochem.* **104,** 846–858
25. Legleiter, J., Mitchell, E., Lotz, G. P., Sapp, E., Ng, C., DiFiglia, M., Thompson, L. M., and Muchowski, P. J. (2010) Mutant huntingtin fragments form oligomers in a polyglutamine length-dependent manner *in vitro* and *in vivo. J. Biol. Chem.* **285,** 14777–14790
26. Sathasivam, K., Lane, A., Legleiter, J., Warley, A., Woodman, B., Finkbeiner, S., Paganetti, P., Muchowski, P. J., Wilson, S., and Bates, G. P. (2010) Identical oligomeric and fibrillar structures captured from the brains of R6/2 and knock-in mouse models of Huntington's disease. *Hum. Mol. Genet.* **19,** 65–78
27. Montie, H. L., Pestell, R. G., and Merry, D. E. (2011) SIRT1 modulates aggregation and toxicity through deacetylation of the androgen receptor in cell models of SBMA. *J. Neurosci.* **31,** 17425–17436
28. Roy, J., Minotti, S., Dong, L., Figlewicz, D. A., and Durham, H. D. (1998) Glutamate potentiates the toxicity of mutant Cu/Zn-superoxide dismutase in motor neurons by postsynaptic calcium-dependent mechanisms. *J. Neurosci.* **18,** 9673–9684
29. Orr, C. R., Montie, H. L., Liu, Y., Bolzoni, E., Jenkins, S. C., Wilson, E. M., Joseph, J. D., McDonnell, D. P., and Merry, D. E. (2010) An interdomain

interaction of the androgen receptor is required for its aggregation and toxicity in spinal and bulbar muscular atrophy. *J. Biol. Chem.* **285,** 35567–35577

30. Mojsilovic-Petrovic, J., Nedelsky, N., Boccitto, M., Mano, I., Georgiades, S. N., Zhou, W., Liu, Y., Neve, R. L., Taylor, J. P., Driscoll, M., Clardy, J., Merry, D., and Kalb, R. G. (2009) FOXO3a is broadly neuroprotective *in vitro* and *in vivo* against insults implicated in motor neuron diseases. *J. Neurosci.* **29,** 8236–8247

31. Merry, D. E., Kobayashi, Y., Bailey, C. K., Taye, A. A., and Fischbeck, K. H. (1998) Cleavage, aggregation, and toxicity of the expanded androgen receptor in spinal and bulbar muscular atrophy. *Hum. Mol. Genet.* **7,** 693–701

32. Diamond, M. I., Robinson, M. R., and Yamamoto, K. R. (2000) Regulation of expanded polyglutamine protein aggregation and nuclear localization by the glucocorticoid receptor. *Proc. Natl. Acad. Sci. U.S.A.* **97,** 657–661

33. Sontag, E. M., Lotz, G. P., Yang, G., Sontag, C. J., Cummings, B. J., Glabe, C. G., Muchowski, P. J., and Thompson, L. M. (2012) Detection of mutant Huntingtin aggregation conformers and modulation of SDS-soluble fibrillar oligomers by small molecules. *J. Huntingtons Dis.* **1,** 127–140

34. Bailey, C. K., Andriola, I. F., Kampinga, H. H., and Merry, D. E. (2002) Molecular chaperones enhance the degradation of expanded polyglutamine repeat androgen receptor in a cellular model of spinal and bulbar muscular atrophy. *Hum. Mol. Genet.* **11,** 515–523

35. Stenoien, D. L., Cummings, C. J., Adams, H. P., Mancini, M. G., Patel, K., DeMartino, G. N., Marcelli, M., Weigel, N. L., and Mancini, M. A. (1999) Polyglutamine-expanded androgen receptors form aggregates that sequester heat shock proteins, proteasome components and SRC-1, and are suppressed by the HDJ-2 chaperone. *Hum. Mol. Genet.* **8,** 731–741

36. Mitra, S., Tsvetkov, A. S., and Finkbeiner, S. (2009) Single neuron ubiquitin-proteasome dynamics accompanying inclusion body formation in Huntington disease. *J. Biol. Chem.* **284,** 4398–4403

37. Ortega, Z., Díaz-Hernández, M., Maynard, C. J., Hernández, F., Dantuma, N. P., and Lucas, J. J. (2010) Acute polyglutamine expression in inducible mouse model unravels ubiquitin/proteasome system impairment and permanent recovery attributable to aggregate formation. *J. Neurosci.* **30,** 3675–3688

38. Rusmini, P., Sau, D., Crippa, V., Palazzolo, I., Simonini, F., Onesto, E., Martini, L., and Poletti, A. (2007) Aggregation and proteasome: the case of elongated polyglutamine aggregation in spinal and bulbar muscular atrophy. *Neurobiol. Aging* **28,** 1099–1111

39. Peters-Libeu, C., Miller, J., Rutenber, E., Newhouse, Y., Krishnan, P., Cheung, K., Hatters, D., Brooks, E., Widjaja, K., Tran, T., Mitra, S., Arrasate, M., Mosquera, L. A., Taylor, D., Weisgraber, K. H., and Finkbeiner, S. (2012) Disease-associated polyglutamine stretches in monomeric huntingtin adopt a compact structure. *J. Mol. Biol.* **421,** 587–600

40. Klein, F. A., Zeder-Lutz, G., Cousido-Siah, A., Mitschler, A., Katz, A., Eberling, P., Mandel, J.-L., Podjarny, A., and Trottier, Y. (2013) Linear and extended: a common polyglutamine conformation recognized by the three antibodies MW1, 1C2 and 3B5H10. *Hum. Mol. Genet.* **22,** 4215–4223

41. Young, J. E., Garden, G. A., Martinez, R. A., Tanaka, F., Sandoval, C. M., Smith, A. C., Sopher, B. L., Lin, A., Fischbeck, K. H., Ellerby, L. M., Morrison, R. S., Taylor, J. P., and La Spada, A. R. (2009) Polyglutamine-expanded androgen receptor truncation fragments activate a Bax-dependent apoptotic cascade mediated by DP5/Hrk. *J. Neurosci.* **29,** 1987–1997

42. Ellerby, L. M., Hackam, A. S., Propp, S. S., Ellerby, H. M., Rabizadeh, S., Cashman, N. R., Trifiro, M. A., Pinsky, L., Wellington, C. L., Salvesen, G. S., Hayden, M. R., and Bredesen, D. E. (1999) Kennedy's disease: caspase cleavage of the androgen receptor is a crucial event in cytotoxicity. *J. Neurochem.* **72,** 185–195

43. Schipper-Krom, S., Juenemann, K., Jansen, A. H., Wiemhoefer, A., van den Nieuwendijk, R., Smith, D. L., Hink, M. A., Bates, G. P., Overkleeft, H., Ovaa, H., and Reits, E. (2014) Dynamic recruitment of active proteasomes into polyglutamine initiated inclusion bodies. *FEBS Lett.* **588,** 151–159